_____

Numerical Simulation of Shedding Pattern of Near Wake Vortices Behind a Circular Cylinder Near a Plane Boundary

Dr. A. K. Singha
Department of Jute and Fibre Technology,
University of Calcutta
35 Ballygunge Circular Road, Kolkata-700 019,
West Bengal, India
e-mail: amiya_singha@rediffmail.com

Abstract— In this paper, flow past a circular cylinder is numerically simulated under the influence of a plane boundary. The vorticity-stream function formulation is used for a wide range of Reynolds numbers consistent of two-dimensional flow. The conventional finite difference implicit scheme is used by implementing the appropriate boundary conditions at all boundaries. The transition from twin vortex regime to vortex shedding regime is studied. The transition is delayed as the gap between the cylinder and wall decreases. The same is because of the interaction between the wake of the cylinder and the boundary wall vorticity. The results are compared with the previous observations of the inhibition of the vortex shedding for body placed inside a channel as well as near a plane wall. The unsteady vortex shedding regime from a pattern similar to the von-karman street when the cylinder is far from the plane wall to a single row of same sign vortices as the body approaches the wall. The separated vortex dynamics leading to this tropological modification is presented.

Keywords- *Incompressible flow; Vorticity, Vortex shedding; Stream function; Circular cylinder; Gap ratio; Finite difference method; Plane wall;*
_____ ***** _____

1. INTRODUCTION

The flow past a circular cylinder is characterized by the cylinder based Reynolds number Re=UD/ν, where U is the free stream velocity, D is the cylinder diameter and ν is the kinematic viscosity.

The incompressible flow of Newtonian fluid around a circular cylinder near a plane boundary is studied in this work.

As the flow takes place past a circular cylinder, the shedding of near wake vortices occurs over a wide range of Reynolds numbers. These types of flow has been found in practical applications like heat exchanger tubes, hot wire anemometers, warm sensors etc.

The most relevant features of the flow, at Reynolds numbers close to 5, the separation of boundary layer on the cylinder surface begins [1]. A pair of steady symmetric vortices develops behind the cylinder between Reynolds numbers 10 to 40 [2]. In this range of Reynolds numbers, re circulation zone length grows linearly with the increase in Reynolds numbers [2]., The instability of the systematic wake occurs at moderate Reynolds number, around 49, followed by a time-periodic regime characteristics by alternate shedding of vortices at cylinder wake whose dimensional period depends on the Reynolds numbers. The shedding of vortices remains laminar for Reynolds number up to approximate 150 [2]. By further increasing Reynolds numbers, a transition to three dimensional flow starts at Reynolds numbers of around 180-194 and ends at Reynolds numbers equal to about 260 depending on experimental condition results in appearance of fine scale three dimensional eddies [3].

Many researchers have studied and investigated the effect of a plane boundary on the hydrodynamic forces, vortex shedding behavior experimentally. Most of the experiments were carried out at the Reynolds numbers in the sub-critical regime up to 1.5×10^{-5} [4]. In this range of Reynolds numbers, the boundary layer is laminar throughout the circumference of the cylinder until separation takes place. In the case of an unbounded cylinder, the vortex shedding is regular and the Strouhal number which measures the vortex shedding frequency remains unchanged. Many experimental work have been reported for the flow around a circular cylinder in the presence of a single plane wall at moderate Reynolds number in a turbulent regime [5-8]. These results have shown that the effects due to the presence of the wall are the modification of the forces on the body as it approaches the wall, a slight variation of Strouhal number, the shedding and vortex shedding suppression when the body is closer than a critical gap ratio G/D, where G is the gap and D is the cylinder diameter. Bearman and Zdravkovich [5] have shown that the wake structure and Strouhal number are about the same as the unbounded case until the cylinder close to the surface such that G/D is as small as 0.3-0.4. At smaller G/D ratio, the wake is almost steady and the periodic shedding is strongly inhibited. Price et al [6] studied the fluid flow around the cylinder using flow visualization, particle image velocimetry and hot-film anemometry for Reynolds number between 1200 and 4960. The effect of changing gap ratio on lift and drag coefficient was studied by Dipankar and Sengupta [7], using an improved overset grid method to compare computed results with [6] for Re=1200 only. Some experimental works in this problem may be found in the paper of Lei et al [8]. This work focused on the dependence of vortex shedding and cylinder forces on the gap ratio. They have shown that the vortex shedding is inhibited at G/D ratio 0.2–0.3. They found that the drag co-efficient Cd increased with increasing gap raios because of the reduction of base pressure. The same trend of base pressure dependence had been observed by Bearman and Zdravkovich [5]. Bearman and Zdravkovich [5] further found that the Strouhal number for G/D $\geq$ 0.3 was more or less constant in their experiments at Re = 4.8×10^{-4}. Lei et al [8] also noted only slight fluctuation in Strouhal number computed from free stream velocity from a similar range of G/D ratios. However for G/D less than 0.3, vortex shedding was suppressed. Bearman and Zdravkovich [5] used a spectral analysis of hot wire signals in the cylinder wake whereas the method of Lei et al [8] was based on observation of the spectrum of the lift coefficient.

_____

Zovatto and Pedriazzeti [9] in his study used a finite element method based on vorticity - stream function formulation to analyze flow around a circular cylinder placed eccentrically between parallel walls. They found that when the body is far enough from one wall, the vortex shedding similar to the Von- Karman vortex street. When the cylinder is closer to one wall, the two layers of opposite sign vorticity separated from the cylinder and from the wall for a pair of vortex which dissipate during the mutual induced stretching. As a result, in a unsteady regime, when the gap between cylinder and one wall smaller than the cylinder diameter the Von- Karman vortex street is substituted by a single row same sign vortices.

Sahin & Owens [10], in their work investigated the lateral wall proximity effects on stability, strouhal number, hydrodynamic forces and wake structure behind the cylinder for a wide range of blockage ratio and Reynolds Number up to 280. Their work differs from the work of Zovatto and Pedrizzetti that they place the cylinder centrally and made the parallel walls closer to each other, whereas Zovatto and Pedrizzetti kept the distance between parallel wall fixed and the cylinder placed eccentrically. Sahin & Owens [10] used a finite volume based method on a velocity only formulation to solve the flow field around a circular cylinder confined in a channel. They found three separate curves of neutral stability, Hopt bifurcation of a symmetric state and Hopt bifurcation of a asymmetric state. Wen and Lin [11] in their experiment, investigated the relationship of two dimensional vortex shedding frequency with the Reynolds number ranging from 45 upto 560. Vortex shedding past a circular cylinder under the influence of buoyancy has been studied by Patnaik et. al. [12]. They have used finite element method with modified velocity correction procedure. They presented the influence of buoyancy on Nusselt number, wake structure etc. They found that at low Reynolds number about Re = 20-40 buoyancy opposing the flow could trigger vortex shedding.

In the present work, the interaction between a laminar stream and a circular cylinder placed over a plane boundary is studied. In this study, the two dimension Navier-Stokes equations are solved in the finite difference implicit method with vorticity - stream function formulation such that continuity equation is satisfied exactly and pressure term is eliminated. This work aims at characteristics of the shedding of near wake vortices as the body approaches the plane wall as the Re varies in the range from the transition to the periodic shedding regime to values where the two-dimensional approximation is represented. The feature of the separated vorticity dynamics are analyzed at different conditions with a vigilances to the interaction between the cylinder wake and the induced separation on the plane walls. The presence of the plane wall influenced the shedding frequencies and their dependence of Re.

2. PHYSICAL FLOW FIELD

The flow domain of interest and boundary conditions are depicted in Figure 1. A rectangular flow field with bottom as solid plane wall, contains a circular cylinder of diameter D, whose position from bottom no-slip wall is defined by the gap G. The cylinder is located at 5D from the inflow boundary. The top lateral boundary is set at 11D from the bottom wall.

The outflow boundary is located at 25D from the cylinder centre.

Consider an incompressible fluid, with density ρ and kinematics viscosity ν, flowing with steady velocity U in the flow domain. The problem is made dimensionless by taking D as unit length, D/U as unit time and ρD^3, as unit mass. The flow is governed by two dimensionless parameter: The Reynolds number and the gap ratio G/D. The gap ratio is a positive number which takes its minimum value zero as the cylinder touches the bottom wall.
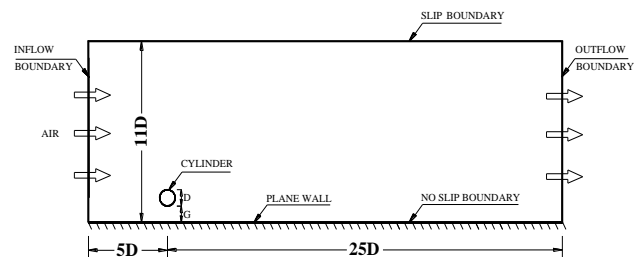
Figure 1 Configuration of the flow field.

3. MATHEMATICAL FORMULATION

In this study a Cartesian systems of co-ordinates (x, y) with x-axis along the bottom wall is considered. The governing equations are the Navier-stokes equations which are written in the vorticity-stream function formulation:

$$\frac{\partial \omega}{\partial t} + u\frac{\partial \omega}{\partial x} + v\frac{\partial \omega}{\partial y} = \frac{1}{\text{Re}}\left(\frac{\partial^2 \omega}{\partial x^2} + \frac{\partial^2 \omega}{\partial y^2}\right) \qquad (1)$$

Vorticity and stream function are related by the poission's equation:

$$\frac{\partial^2 \Psi}{\partial x^2} + \frac{\partial^2 \Psi}{\partial y^2} = -\omega \qquad (2)$$

Where ω is the vorticity, ψ is the stream function and u, v denotes the components of velocity in x and y direction, which can be calculated from the stream function:

$$\frac{\partial \Psi}{\partial y} = u \qquad \frac{\partial \Psi}{\partial x} = -v \qquad (3)$$

4. NUMERICAL METHOD

In order to solve the governing equation in a curvilinear co-ordinate system, the following co-ordinate transformation is used:

$$\xi = \xi(x,y), \quad \eta = \eta(x,y) \qquad (4)$$

where (ξ, η) is the co-ordinate system in the computational plane. Using above transformation, the derivatives in the physical and computational plane are related as follows:

3150

_____

The Laplace equations used as the generation system are:

$$\xi_{xx} + \xi_{yy} = P(\xi, \eta) \tag{5}$$

$$\eta_{xx} + \eta_{yy} = Q(\xi, \eta) \tag{6}$$

These equations are transformed to (ξ, η) co-ordinates by interchanging the roles of dependent and independent variables which results following elliptic system of equations:

$$Ax_{\xi\xi} - 2Bx_{\xi\eta} + Cx_{\eta\eta} = -J^2(Px_\xi + Qx_\eta) \tag{7}$$

$$Ay_{\xi\xi} - 2By_{\xi\eta} + Cy_{\eta\eta} = -J^2(Py_\xi + Qy_\eta) \tag{8}$$

where,
$$A = x_\eta^2 + y_\eta^2$$
$$B = x_\xi x_\eta + y_\xi y_\eta$$
$$C = x_\xi^2 + y_\xi^2$$
and
$$J = x_\xi y_\eta + x_\eta y_\xi \ \square$$
$$\square\square\square\square\square\square\square\square\square\square\square\square\square\square\square\square\square \tag{9}$$

where J is the Jacobian of transformation.

The source terms P and Q in equations (5) and (6) are considered according to Thomas and Middlecoff [13].

$$P = \phi(\xi, \eta)(\xi_x^2 + \xi_y^2) \tag{10}$$
$$Q = \varphi(\xi, \eta)(\eta_x^2 + \eta_y^2) \tag{11}$$

Now the vorticity – transport equation (1) in the computational plane are rewritten as:

$$\alpha\omega_{\xi\xi} + 2\beta\omega_{\xi\eta} + \gamma\omega_{\eta\eta} + \delta\omega_\xi + \varepsilon\omega_\eta = \\ \mathrm{Re}[u(\omega_\xi\xi_x + \omega_\eta\eta_x) + v(\omega_\xi\xi_y + \omega_\eta\eta_y)] + \mathrm{Re}\,\omega_t \tag{12}$$

The stream function equation (2) in the computational plane is rewritten as:

$$\alpha\psi_{\xi\xi} + 2\beta\psi_{\xi\eta} + \gamma\psi_{\eta\eta} + \delta\psi_\xi + \varepsilon\psi_\eta = -\omega \tag{13}$$

The velocities are rewritten as:
$$u = \xi_y\psi_\xi + \eta_y\psi_\eta \qquad v = -(\xi_x\psi_\xi + \eta_x\psi_\eta) \tag{14}$$

5. BOUNDARY CONDITIONS AND INITIAL CONDITIONS

In this study, inflow boundary is specified with an uniform longitudinal free stream velocity U, and zero transverse velocity which is equivalent to impose the boundary for stream function with $\psi = U \cdot y$ and vorticity $\omega = 0$. No-slip boundary conditions are imposed on wall and cylinder surfaces.

The no slip boundary conditions for vorticity at cylinder surface and wall can be written as per Thom's formula [14],

$$\omega_{i,0} = \frac{2(\psi_{i,1} - \psi_{i,0})}{(y_{i,1} - y_{i,0})^2} \qquad \text{at bottom wall} \tag{15}$$

$$\omega_{ic,jc} = \frac{2(\psi_{ic,jc} - \psi_{ic,jc-1})}{h_{ic,jc}^2} \qquad \text{at cylinder surface} \tag{16}$$

where (ic, jc) denotes the nodes on the cylinder surface and $h_{ic,jc}$ is the radial distance between cylinder surface and first body fitted node around the cylinder.

The no slip boundary condition is applied at the cylinder surface ie the velocity of the fluid is equal to zero on the surface of the cylinder. In the multiply connected domain, the value of stream function at the surface of cylinder is an unknown constant and vary with time. This constant must be determined and updated at each time step during computation. To calculate the value of stream function on the cylinder surface Liu Jian-Guo et al [15] suggested the use of the single valued condition of the pressure for the multiply connected domain. The pressure single-value condition is derived from the fact that the pressure is a scalar term.

6. NUMERICAL SOLUTIONS.

In this study Thompson, Thames, Mastin (TTM) method of generation of automatic boundary fitted co-ordinate generation system is used to construct the grids of the physical flow field. The numerical results were obtained by the solution of equations by finite difference method. The mesh dependence study of an unbounded cylinder shows that considerable accurate results can be obtained with a 244 x 90 mesh with 72 node in the circumferential direction. Grid around the cylinder and wall is refined with care. The typical size of smaller grid is considered as 0.002 and time step is considered as 0.002 to satisfy CFL condition.

The transformed equations in computational plane are solved numerically by tri-diagonal matrix algorithm in finite difference implicit method. The iterative process is carried out to reach the steady convergence. The first order backward in time and second order central in space finite difference method is used. The relaxation factor 0.2-0.5 is employed to promote smooth convergence.

The following convergence criteria was used for the computations,

$$\left| \frac{f^n - f^{n-1}}{f^n} \right| \le 0.0002 \tag{17}$$

where f represents $\omega, \psi, u, v \,\&\, \theta$ and n is the iteration number.

7. RESULTS AND DISCUSSION

Based on the above mentioned solution method a computer code is developed. The discretization process involves a certain amount of error which can be systematically reduced by grid refinement.

3151

_____

Figure 2 presents the mesh of the flow domain for a gap ratio of G/D = 0.5. By (244 x 90) mesh, it is implied that there are 244 nodes in the longitudinal and 90 nodes in the transverse direction, respectively, with 72 nodes on cylinder surface. In this study, calculations are performed with a non-dimensional time step of t = 0.002. The vorticity-transport equation is solved through second order central difference scheme. Stream function equation is solved through central difference.
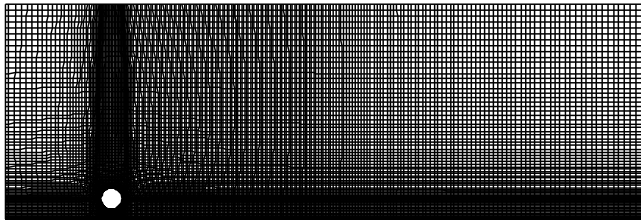
Figure 2 Mesh of the flow domain for a gap-ratio of G/D = 0.5.

7.1 Flow about a circular cylinder near a plane wall

The flow about a circular cylinder in an unbounded domain has been discussed and flow feature has been explained. The solution is validated against the solutions from the other researchers. Good agreements are shown with the previous researchers.

The flow about a cylinder near a plane wall differs from its unbounded counterpart because of the effect of wall and shear in the incoming velocity profile and separation of vorticity from the wall. The case of a circular cylinder placed near a plane wall is studied numerically with the method discussed above.

7.2.1 Vortex shedding

To explain the interaction of wall boundary layer with the cylinder, a Reynolds number of 100 has been chosen for a gap ratio of G / D = 0.5 where G is the gap between the cylinder and the wall and D is the diameter of the cylinder. Time-dependent behavior of streamlines and the mechanism of vortex shedding over a typical time cycle for G/D = 0.5 and Re = 100 is shown in Figure 3. The non-uniformity of streamlines around the cylinder strongly suggests the possibility of such an interaction.

The flow pattern around the cylinder is essentially periodic in nature i.e. a typical flow pattern is repeated after a fixed interval of time. If the flow in the upstream region of the unbounded cylinder is carefully observed, it will be seen that flow varies about the upstream divider streamline i.e. for half of the time period, there is crowding of the streamlines below the divider streamline, only to be followed later by expansion of the same. The same happens for flow above the divider streamline. It appears that during the whole time period, the divider streamline also changes its spatial position keeping the forward stagnation point apparently fixed. This time dependent flow dissimilarity in the upstream region of the cylinder is deemed to be responsible for temporal and spatial variation in flow quantities in the wake region leading to the phenomenon of "vortex shedding". However, in this context, the proximity of the cylinder to a stationary plane is instrumental in introducing a bias in "flow switching", in the upstream region.

It is observed from Figure 3 that the movement of the divider streamline is now restricted between its time mean position (horizontal) and a slightly higher position compared to the time mean position. Since the "flow switching" in the upstream region is not symmetrical, the possibility of alternate vortex shedding does not arise. It now appears to be interesting to examine what happens in the wake region of the cylinder, particularly, against the backdrop of "biased" flow switching in the upstream region (refer Figure 3). At t = 0, streamlines, in the bottom half of the upstream region are "widening". This expansion of streamlines continue up to about t = 2τ/6. This leads to gradual increase in pressure in the bottom region at the wake of the cylinder. Consequently, streamlines at the bottom try to reach out the upper wake of the cylinder (ref. Figure 3 at t = τ/6). Due to strong curvature of the streamline, a small amount of fluid becomes entrapped between these streamlines and the cylinder (Ref Figure 3 at t = 2τ/6). As the streamlines in the upstream region gradually switches over to the compaction mode, the fluid velocity in the bottom wake region increases and pressure decreases. This lead to further re-structuring of streamlines in the wake and the entrapped region of fluid now moves away from the cylinder.

t = 0

t = 𝜏/6

t = 2𝜏/6

t = 3𝜏/6

t = 4𝜏/6

t = 5𝜏/6

t = 6𝜏/6
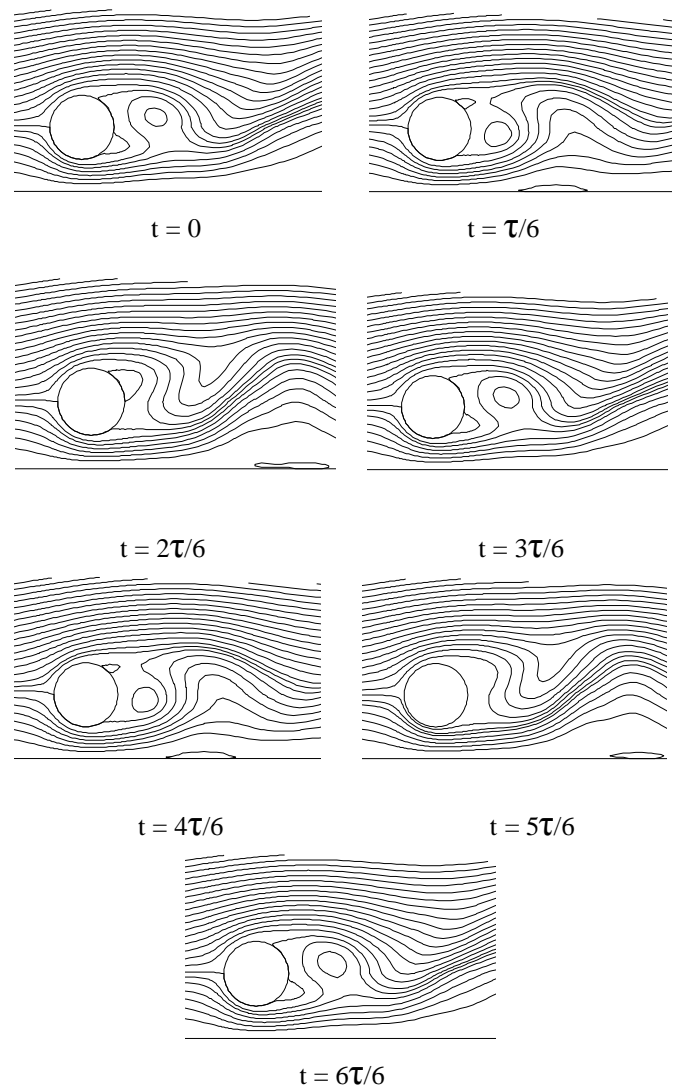
Figure 3 Vortex shedding around the cylinder in a time cycle for Re = 100, G/D = 0.5.

_____

_____

7.2.2 Vorticity isolines

Figure 4 presents the vorticity contour plots for the Reynolds number Re = 150 and for G/D = 2.0,1.5,1.0, 0.8, 0.5, 0.3. The positive (solid lines) and negative (dotted lines) vorticity contours are shown from values ±1 with a constant increase of ± 1 units for all the plots of different Reynolds numbers. The clockwise negative vorticity (dotted line) and anti- clockwise positive vortices (solid line) shed from the upper and lower surface of the cylinder and is convected in the downstream side. At gap ratios G/D = 2.0, 1.5, 1.0, 0.8, the structure of vorticity fields are analogous to the classic von Karman vortex street. The clockwise negative vortices sheds from upper side of the cylinder occupy the upper portion of the street and the anti clockwise positive vortices sheds from the lower side of the cylinder occupy the lower portion of the street. For these gap-ratios, two rows of vortices (clockwise and anti-clockwise) are shed alternatively from the top and bottom surfaces of the cylinder. In this gap ratios, the wall effect is seems to be not very significant. For the gap-ratios G/D = 0.5 and 0.3, shedding of single row of vortices occur from the surface of the cylinder. In fact, at these gap-ratios, relatively stronger and well defined negative vortices are shed only from the upper surface of the cylinder; leaving behind a single row of vortex street in the flow field. The single row of vortex street for the Reynolds number

vortex that is about to shed from the bottom surface of the cylinder at these gap-ratios is being counteracted by the negative wall vorticity. In other words, the cylinder is unable to shed vortices from the lower surface of the cylinder while the vortex from the upper part of the cylinder is shed at regular interval as evident from Figure 4.

The vorticity contours for flow in the steady-state regimes is presented in Figure 5, at Re = 40. Figure 5 presents vorticity contour for Re = 40, and (a) G/D = 2.0, (b) G/D = 1.5, (c) G/D = 1.0, (d) G/D = 0.5. The positive (solid lines) and negative (dotted lines) vorticity contours are shown from values +/- 1 with a constant increase of +/- 1 units. In this steady flow regime where vortex shedding does not occur, the wake vorticity generates at the upper wall is negative and the same generates at the lower wall is positive. When the cylinder is placed far from the wall ie at gap ratio G/D = 2.0, the positive wake vorticity on the wall side elongates due to wall effect. As the cylinder approaches the wall, the wake vorticity on the wall side reduced in length. On the opposite face of the cylinder the wake elongates, smooths out and eventually combines with the oncoming vorticity. Decreasing the gap value, it can be seen that the wall - side wake couples with the wall boundary - layer vorticity of opposite sign while the actual wake is dominated by the vorticity shed from other side of the body. When G/D = 0.5, the wall side wake has almost disappeared and the wake flow resembles that of a surface mounted obstacle.

(a) (b) (c) (d) (e) (f)
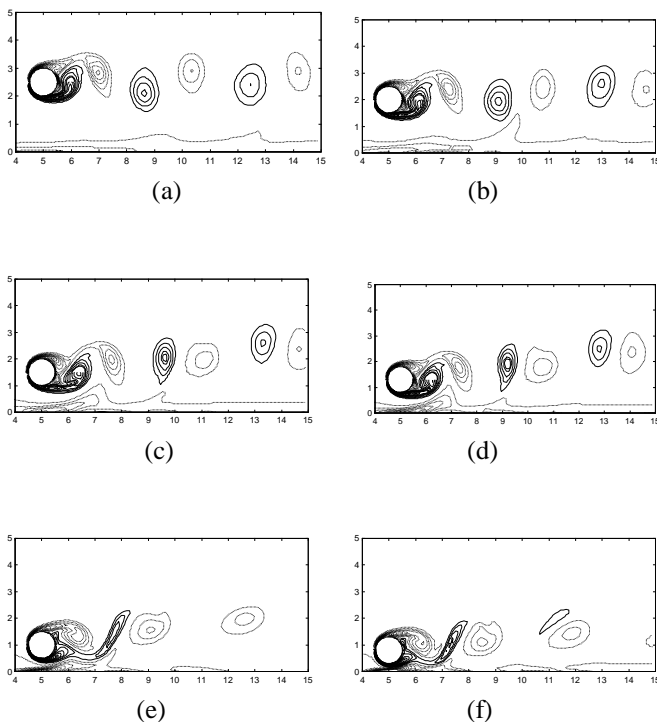
Figure 4 Vorticity contours for Re = 150 and gap-ratios: (a) G/D = 2.0, (b) G/D = 1.5, (c) G/D = 1.0, (d) G/D = 0.8 (e) G/D = 0.5, (f) G/D = 0.3.

Re = 150 and for a gap-ratio of G/D = 0.5 and 0.3 corroborate this nature shown in Figure 4. The weaker positive

(a) (b) (c) (d)
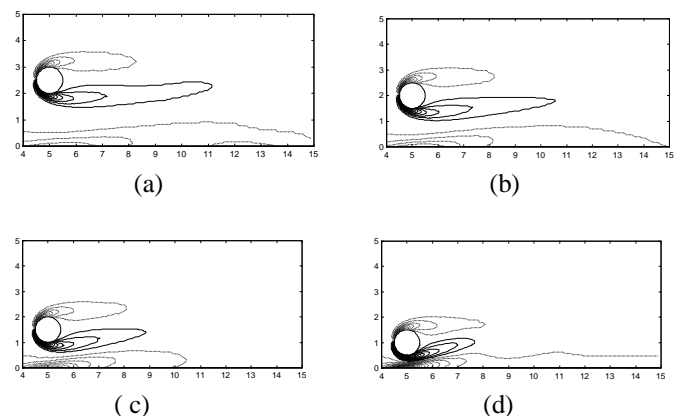
Figure 5 Vorticity contour for Re = 40, and (a) G/D = 2.0, (b) G/D = 1.5, (c) G/D = 1.0, (d) G/D = 0.5.

7.2.3 Velocity Vectors

Figures 6 presents the velocity vectors at Re =100 and 200 for gap ratios G/D = 0.5. The plots clearly show the periodic nature of the flow pattern at the wake. The velicity lines clearly depicted the shedding pattern for Re=100 and Re=200 at the same gap ratio i.e. G/D = 0.5.

_____

_____
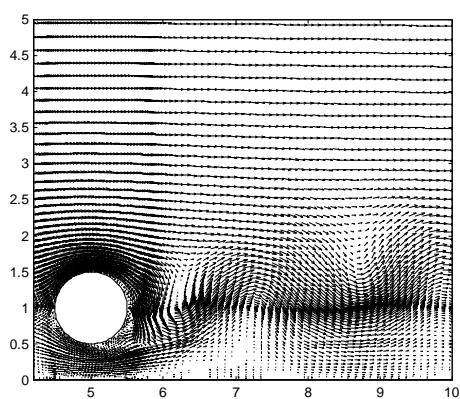
(a)
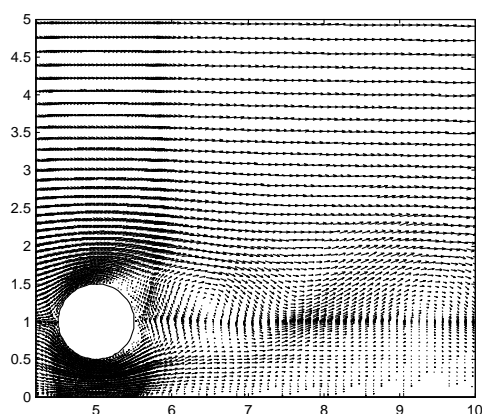
(b)

Figure 6 Velocity vectors G/D = 0.5, and (a) Re = 200, (b) Re = 100.

8. CONCLUSIONS

The studies presented in this paper is relate to the shedding pattern of near wake vortices for flow past a circular cylinder in the vicinity of a plane wall. A non-isothermal case is considered for the flow a fluid is considered to flow past a circular cylinder near a plane wall.

In this work, the two dimensional Navier-Stokes equations for time-dependent, viscous, incompressible flow along with continuity and energy equation are solved using vorticity-stream function formulation by finite difference method.

The major conclusions are as follows:

The time-evolution of cylinder surface stream function also provides a measure of frequency of vortex shedding (Strouhal number) from the cylinder.

The time dependent behavior of the stream function at the surface of the cylinder reveals that the magnitude of variation grows up as the Reynolds number increases; at the same time,

the time period for a cycle decreases, implying that vortices are now shed with greater frequency

Thermal boundary growth starts at the front stagnation and becomes thicker towards the aft. On the upstream side, the distribution is regular and packed, while in the downstream, the migration of these isotherms indicates the vortex shedding.

For relatively higher gap-ratios, shedding of vortices takes place from either surface of the cylinder. The negative vortices sheds from upper surface of the cylinder and the positive vortices sheds from the lower surface of the cylinder. For smaller gap ratios, the flow field changes considerably. There is shedding from one side of the cylinder and from the other side. The positive vortices ceases to sheds from the lower surface of the cylinder due to the interaction with the negative vortices at the wall.

9. REFERENCE:

[1] S. Taneda, "Experimental investigation of the wakes behind cylinders and plates at low Reynolds numbers," Journal of Physical Society of Japan, vol. 11, 1965, p 302.

[2] P. Beaudan, P. Moin, "Numerical Experiments on the flow past a circular cylinder at sub-critical Reynolds number," Report no TF-62, Department of Mechanical Engineering, Standford University, Standford, California, USA, 1994.

[3] C. H. K. Williamson, "Vortex dynamics in the cylinder wake," Annual review of Fluid Mechanics, vol. 28, 1996, pp 477-539.

[4]   H. J. Niemann, N. Holscher, "A review of recent experiments on the flow Past circular cylinders," Journal of Wind Engineering and Industrial aerodynamics, vol. 33, 1990, pp 197- 209.

[5] P. W. Bearman, M. M. Zdravkovich, "Flow around a circular cylinder near a plane boundary," Journal of Fluid Mechanics, vol. 89 (1), 1978, pp. 33-47.

[6]   S. J. Price, D. Summer, J. G. Smith, K. Leong, M. P. Paidoussis, "Flow visualization around a circular cylinder near a plane wall, Journal of fluid and Structures, vol. 16(2), 2002, pp. 175-191.

[7]   A. Dipankar, T. K. Sengupta, "Flow past a circular cylinder in the vicinity of a plane wall," Journal of fluid and structures, vol. 20, 2005, pp. 403-423.

[8] C. Lei, L. Cheng, K. Kavanagh, "Re-examination of the effect of a plane boundary on force and vortex shedding of a circular cylinder," J of Wind Engineering and Industrial Aerodynamics," vol. 80, 1999, pp. 263-286.

[9]. L. Zovatto, G. Pedrizzetti, "Flow about a circular cylinder between parallel walls," Journal of Fluid Mechanics, vol. 440, 2001, pp. 1-25.

[10] M. Sahin, R. G. Owens, "A numerical investigation of wall effects up to high blockage ratios on two dimensional flow past a confined circular cylinder," Physics of Fluids vol.16(5), 2004, pp.1305-1320.

[11] C. Y. Wen, C. Y. Lin, "Two dimensional vortex shedding of a circular cylinder," Physics of Fluids, vol.13(3), 2001, pp. 557-560.

[12] B.S.V.P. Patnaik, K. N. Seetharamu, P. A. Aswatha Narayana, "Simulation of laminar confined flow past a circular cylinder with integral wake splitter involving heat transfer," International Journal of Numerical Methods for Heat and Fluid Flow, vol. 6(4), 1996, pp.65 – 81.

[13] P. D. Thomas, J. F. Middlecoff, "Direct control of the grid point distribution in meshes generated by elliptic equations," AIAA journal, vol. 18, 1980, pp. 652-656.

[14] A. Thom, "The flow past circular cylinder at low speeds," Proc R Soc London Sect A, vol. 141, 1933, pp. 651-69.

[15] Jian-Guo Liu, Cheng Wang, "High order finite difference methods for unsteady incompressible flows in multi-connected domain," Computers & Fluids, vol. 33, 2004, pp. 223.